Published online 2020 September 30 **Original Article**

High-Resolution Computed Tomography in the Differential Diagnosis between Imported COVID-19 and Seasonal Influenza Pneumonia

Yuange Li[1], Shiliang Long[2], Yue Zhao[2], Zhan Ge[1], Weiquan Wu[3,*] and Jun Xia[1]

[1] Radiology Department, Affiliated Hospital of Guangdong Medical University, Zhanjiang, Guangdong, China
[2] Radiology Department, Central People's Hospital of Zhanjiang, Zhanjiang, Guangdong, China
[3] Clinical Research Center, Affiliated Hospital of Guangdong Medical University, Zhanjiang, Guangdong, China

*** *Corresponding author:*** Weiquan Wu, Clinical Research Center, Affiliated Hospital of Guangdong Medical University, Zhanjiang, Guangdong, China. Tel: +8613542006215; Email: 448650702@qq.com

Received 2020 August 01; **Revised** 2020 August 05; **Accepted** 2020 September 21.

Abstract

Background: Nowadays, the world is facing COVID-19 pandemic, and seasonal influenza is also sweeping the world. Therefore, it is essential to make an early differential diagnosis between imported COVID-19 and seasonal influenza pneumonia.

Objectives: The present study aimed to determine the diagnostic value of high-resolution computed tomography (HRCT) imaging characteristics for imported coronavirus disease 2019 (COVID-19) and seasonal influenza pneumonia.

Methods: The HRCT imaging features with 22 cases of imported COVID-19 and 39 cases of seasonal influenza pneumonia were retrospectively analyzed in the current study. The patients with COVID-19 or influenza were diagnosed according to the World Health Organization guidelines and were confirmed following positive reverse transcription-polymerase chain reaction(RT-PCR) analysis of respiratory secretion samples.

Results: Both imported COVID-19 and influenza demonstrated multiple lesions. In the former, the lesions were mostly distributed in the subpleural of peripheral lung (90.9%), and some of them showed an anti-butterfly wing sign (18.2%; P<0.05). In the latter, the lesions were distributed around the bronchial vascular tree with subpleural lesions in peripheral lung (33.3%); nonetheless, they were fewer than those observed in the former (P<0.05). There were some differences in ground-glass opacity (GGO) (95.5% vs. 66.7%, respectively, P<0.05), consolidation (68.2% vs. 12.8%, respectively, P<0.05), and crazy paving sign (86.4% vs. 10.3%, respectively, P<0.05). The air bronchogram sign in the former appeared earlier than those in the latter. When both GGO lesions were mixed, the latter had more solid areas and higher density.

Conclusion: The different chest HRCT features of COVID-19 and seasonal influenza pneumonia can provide considerable evidence for the early diagnosis of imported COVID-19 and seasonal influenza pneumonia and can be of great help for the prevention and control of COVID-19.

Keywords: CT, Influenza, Novel coronavirus, Pneumonia

1. Background

Since first identified in Wuhan, China, in December 2019, there have been multiple cases of novel coronavirus pneumonia which was named coronavirus disease 2019 (COVID-19) by the World Health Organization (WHO) on February 11, 2020 (1, 2). As an acute respiratory infectious disease, the main clinical symptoms of COVID-19, caused by severe acute respiratory syndrome coronavirus 2 (SARS-CoV-2), include fever, dry cough, and fatigue. SARS-CoV-2, which belongs to the β-type coronaviruses, has a polymorphic envelope, and its particles are round or oval with a diameter from 60-40 nm (3-5).

Influenza is a rapid infectious respiratory seasonal disease caused by influenza viruses (6-8). Typical clinical manifestations of this disease are fever, general pain, marked weakness, and respiratory symptoms. Influenza viruses can be classified into A, B, C, and D types (9). At the present time, influenza A and B viruses are responsible for the majority of human infections (10).

Currently, the world is facing a COVID-19 pandemic(11, 12), and seasonal influenza is also sweeping across the world (13, 14). More importantly, the clinical symptoms of both diseases are very similar. Reverse transcription-polymerase chain reaction (RT-PCR) is the gold standard for the diagnosis of both diseases; nonetheless, it requires a long time, high numbers of testing personnel, as well as related testing equipment and technology. In addition, false-negative RT-PCR results can occur as the result of sampling location and other factors (15, 16). As an important complement to RT-PCR (17), high-resolution computed tomography (HRCT) can play a key role in the diagnosis of COVID-19 (18, 19).

2. Objectives

The provision of a basis for the early differential diagnosis between imported COVID-19 and seasonal influenza pneumonia would be of great help in the prevention and control of COVID-19. Therefore, the present study retrospectively analyzed the HRCT imaging features of patients with imported COVID-19 and seasonal influenza pneumonia. It aimed to determine the diagnostic value of HRCT imaging characteristics for imported COVID-19 and seasonal

influenza pneumonia.

3. Methods

3.1. Patient Population

For the purpose of the study, 22 cases (age range: 23-79 years) of imported COVID-19 were diagnosed in the Affiliated Hospital of Guangdong Medical University and Central People's Hospital of Zhanjiang from January 19, 2020 to February 24, 2020. The majority of the patients were male (n=12). The patients with COVID-19 were diagnosed according to the WHO guideline and were confirmed following positive RT-PCR analysis of respiratory secretion samples. All COVID-19 patients underwent HRCT examination. Except for one clinically asymptomatic patient, other patients had fever onset (n=21), dry cough (n=16), fatigue (n=7), diarrhea (n=2), vomiting (n=1), and headache (n=2). The following underlying diseases were reported: a history of hypertension or coronary heart disease (n=6) and a history of hyperglycemia (n=3)

On the other hand, 39 cases (age range:1-77) of influenza were diagnosed in the Emergency Department of the Affiliated Hospital of Guangdong Medical University from January 19, 2020 to February 24, 2020. The patients with influenza were diagnosed according to the WHO guideline and were confirmed following positive RT-PCR analysis of respiratory secretion samples (type A=14 cases, type B=22 cases, type A+B=3 subjects). All patients with influenza underwent HRCT examination. It is noteworthy that the majority of subjects were male (n=26). The following underlying diseases were reported in the patients: a history of hypertension (n=9), a history of hyperglycemia (n=5), coronary heart disease (n=4), lung cancer (n=1), esophageal cancer (n=1), renal failure (n=1). The study was approved by the Ethics Committee of the Affiliated Hospital of Guangdong Medical University. Written informed consent was received from all patients. During and after data collection, all authors obtained information that could identify individual participants.

3.2. Imaging Methods

The patients underwent HRCT scans, consisting of a GE 64-slice spiral CT or Siemens 16-slice CT. General HRCT parameters were as follows: layer thickness and spacing=8 mm, tube voltage=100-20 kV, and tube current= 250-350 mAs. After scanning, the conventional high-resolution thin layer images with layer thickness and spacing of 0.5-1 mm were reconstructed. CT rescanning was performed at intervals of 3-5 days, and the dynamic changes in imaging characteristics were analyzed.

3.3. Image Analyses

The CT images were analyzed by two chief physicians with considerable experience in diagnostic imaging, and the image manifestations of the lesions were described. In the case of different opinions, they reached a consensus through negotiation.

3.4. Statistical Analyses

The data were analyzed in SPSS software (version 17.0) (SPSS Inc., Chicago, IL, USA). The independent-sample *t*-test was used to investigate the age differences of the patients with COVID-19 and subjects with influenza. Moreover, gender differences between COVID-19 patients and those with influenza were assessed using Fisher's exact test. Furthermore, the distribution and manifestations of lesions on HRCT between COVID-19 and influenza were analyzed using Fisher's exact test. A p-value less than 0.05 was considered statistically significant.

4. Results

4.1. CT Manifestations of COVID-19

22 COVID-19 patients had characteristic chest CT manifestations on CT scanning. Regarding lesion distribution, 2 (9.1%), 19 (86.4%), and 20 (90.9%) cases had lesions in a single lung lobe segment, multiple lung lobe segments, and under the pleura outside the lung band accounting for the majority of cases, respectively.

Regarding lesion manifestations, the first CT scan demonstrated the followings: pure ground-glass opacity (GGO) (n=2, 9.1%) mixed GGO (n=19, 86.4%) (Figure 1), consolidation (n=8, 36.4%) , a crazy paving sign (n=18, 81.8%) , thickening of blood vessels in the lesions (n=17,77.3%) (Figure 2), an air bronchogram sign which appeared early(n=16, 72.7%) , anti-butterfly wing sign (n=4, 18.2%) (P<0.05)(Figure 3), and three cases (13.6%) showed fibrous strip shadows. The results of the second CT scan were as follows: disappearance of CT lesions (n=2,9.1%), GGO alone (n=1, 4.5%) , mixed GGO (n=18, 81.8%), consolidation (n=12, 54.5%), a crazy paving sign (n=19, 86.4%) , thickening of blood vessels in the lesions (n=15, 68.2%) , an air bronchogram sign (n=13 cases, 59.1%), an anti-butterfly wing sign (n= 4, 18.2%), and fibrous strip shadows(n=5, 22.7%) (3). The third CT scan showed: consolidation (n=15, 68.2%) , increased fibrous strip shadows (n=17, 77.3%), a crazy paving sign (n=5, 22.7%), an air bronchogram sign (n=7, 31.8%), and a decrease in the anti-butterfly wing sign (n=1, 4.5%) .

Other manifestations were as follows: pleural thickening (n=10 , 45.5%), lymphadenopathy (n=2, 9.1%), and pleural effusion (n=3, 13.6%).

4.2. Computed tomography Manifestations of Influenza

Out of 39 patients with influenza, 8 cases showed negative CT findings. The CT manifestations in 31 of 39 influenza patients were as follows: 25 (64.1%) cases showed multiple lung field lesions, and six

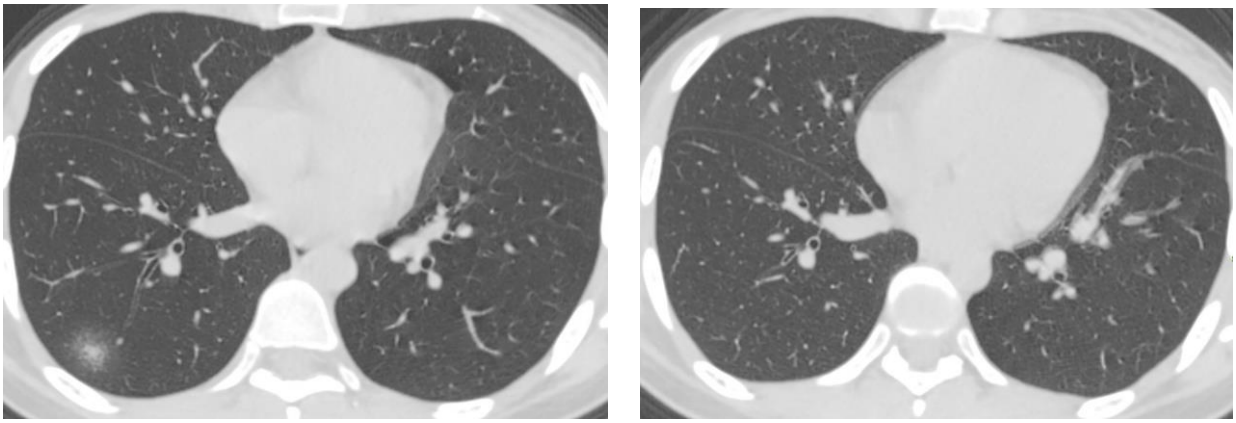

(A) (B)

Figure 1. A 24-year-old female patient COVID-19. The first computed tomography scan showed mixed GGO with very few solid areas (A). After 10 days, the lesions disappeared (B).

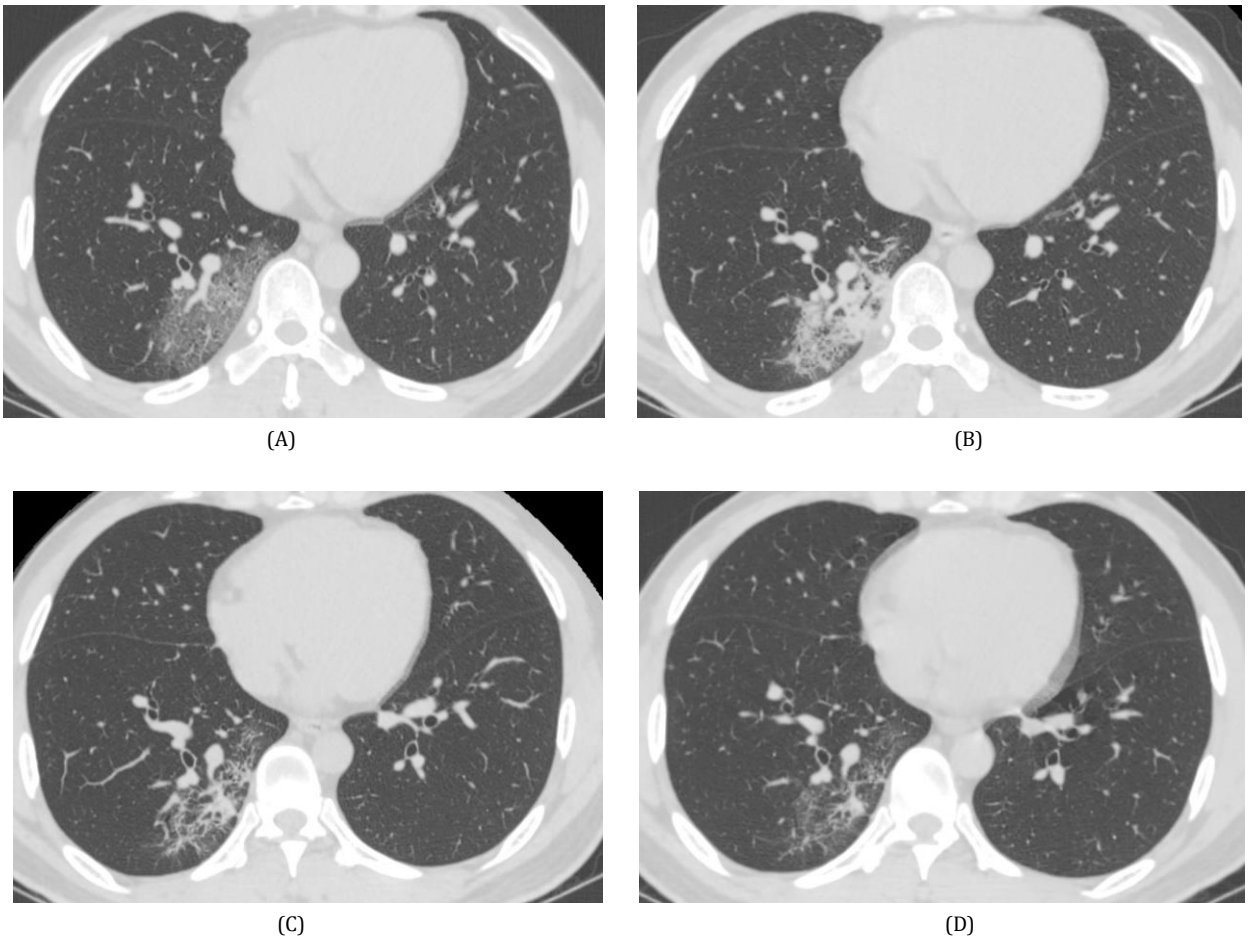

(A) (B)

(C) (D)

Figure 2. A 42-year-old male patient with COVID-19. The first computed tomography scan demonstrated flaky GGO with thickened blood vessels and slightly thicker leaflet intervals (A). The second computed tomography scan showed thickened lobular intervals, a typical crazy-paving sign, and the solid area had increased (B). The third and fourth computed tomography scans showed that the lesions were mainly fibrous strip shadows (C-D).

(15.4%) subjects demonstrated unilateral lesions. Regarding lesion distribution, 15 (38.5%) and 12 (30.8%) cases had lesions along the vascular bundle in the inner zone of the lung field and under the pleura outside the lung band; however, they were fewer than those observed in COVID-19 patients ($P<0.05$). Moreover, 12 (30.8%) and 14 (35.9%) cases showed pure GGO(Figure 4) and mixed GGO,

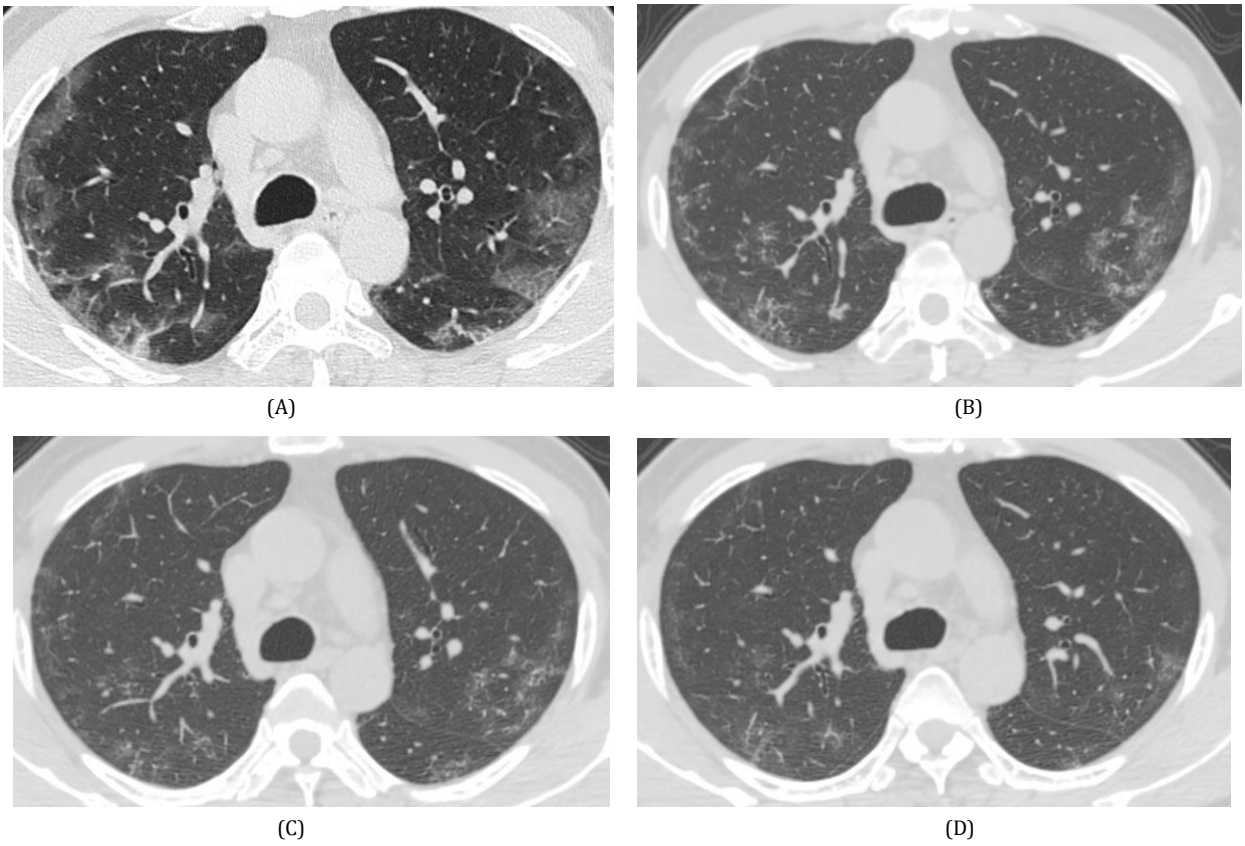

Figure 3. A 54-year-old male patient with COVID-19. The first computed tomography scan showed the anti-butterfly wing sign (A). From the first to third computed tomography scan, the lesions gradually decreased (B-D).

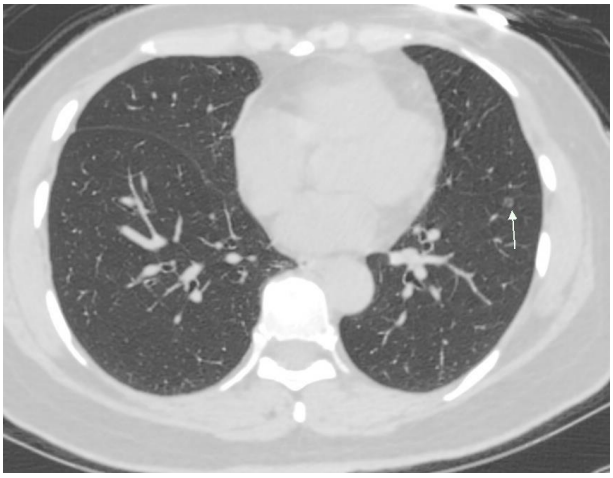

Figure 4. A 47-year-old female patient with influenza B. Computed tomography scan showed simple ground-glass opacity (indicated by arrows).

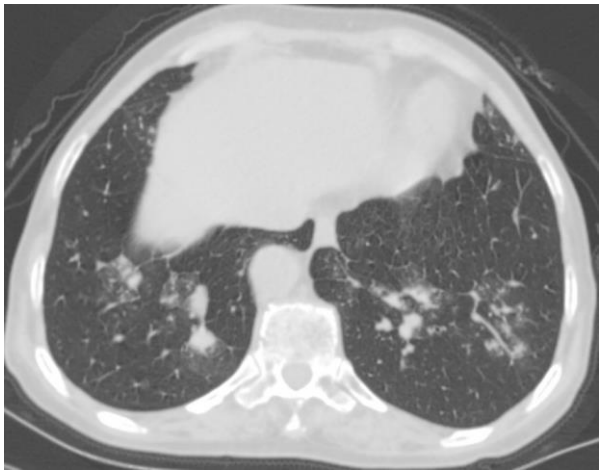

Figure 5. A 59-years-old female patient with influenza A. CT scan demonstrated multiple mixed ground-glass opacity along the bronchial vascular bundle with many solid components and high density.

respectively; nonetheless, they were less than that reported in COVID-19 patients (P<0.05). Although more solid areas with higher density were observed (Figure 5), 5 (,12.8%) cases demonstrated consolidation but less than that detected in COVID-19 patients (P<0.05). Moreover, 4 (10.3%) subjects showed a crazy-paving sign but less than that reported in COVID-19 patients (P<0.05). In addition, 20 (51.3%) cases demonstrated an air bronchogram sign in lesions which appeared later than the signs in

Table 1. Comparison of computed tomography characteristics in patients with COVID-19 and influenza pneumonia

Characteristics	COVID-19 (n=22)	Influenza Pneumonia (n=39)	P-value
Age (years)			
Mean	40.5	31.9	0.116
Range	23-79	1-77	
Sex, n (%)			
Male	12 (54.5)	26 (66.7)	0.415
Female	10 (45.5)	13 (33.3)	
Distribution of lesions, n (%)			
Multiple lesions	19 (86.4)	25 (64.1)	0.079
Outside band	20 (90.9)	12 (30.8)	< 0.001
Manifestations of lesions, n (%)			
ground-glass opacity (GGO)	21(95.5)	26(66.7)	0.011
Consolidation	15(68.2)	5(12.8)	< 0.001
Crazy paving sign	19(86.4)	4(10.3)	< 0.001
Air bronchogram sign	16(72.7)	20(51.3)	0.115
Anti-butterfly wing sign	4(18.2)	0(0)	0.014
Fibrous strip shadows	17(77.3)	25(64.1)	0.391
Pleural thickening	10(45.5)	17(43.6)	1.000
Lymphadenopathy	2(9.1)	5(12.8)	1.000
Pleural effusion	3(13.6)	3(7.7)	0.658

COVID-19 patients, and 25 (64.1%) patients showed fibrous strip shadows. Other manifestations were lymphadenopathy (n=5, 12.8%), a small amount of pleural effusion (n=3, 7.7%), and pleural thickening (n=17 , 43.6%).

The CT characteristics in patients with COVID-19 and influenza pneumonia are displayed in Table 1.

5. Discussion

The major clinical symptoms of COVID-19 and influenza are similar; nonetheless, their prevention and control measures, as well as treatments are different. Therefore, the rapid and differential diagnosis between COVID-19 and influenza is of utmost importance for the prevention and control of epidemics. As a rapid and sensitive method for diagnosing COVID-19 and influenza pneumonia, HRCT can accurately detect small structures, such as bronchioles and lung lobules (20, 21).

5.1. Computed Tomography Dynamic Evolution Manifestations of COVID-19

CT reexaminations were performed on 22 COVID-19 patients 3-5 days after the first CT scan. The dynamic changes observed were as follows: Early-stage: the lesions were mainly multi-lobed and multi-segmental with a few single lesions. The main manifestations were patchy, nodular, fan-shaped, or wedge-shaped GGO in the lung field, and the leaflet interval was slightly thickened. A crazy-paving sign was observed with internal blood vessels slightly thickened and few internal solid areas. Due to earlier damage to alveolar tissue in the lower respiratory tract by the virus, these changes may be attributed to the damage which was inflicted on the interstitial lung and caused an inflammatory reaction in blood vessels in the diseased area. Moreover, in the progression stage, the lobular septum in the diseased area was obviously thickened and showed a typical crazy-paving sign. In addition, the lesions became conspicuous, and some were thickened adjacent to the pleura suggesting alveolar and interstitial damages caused by a significant increase in fluid exudation. Finally, in the recovery period, due to complete absorption, the lesions became less solid with increased clear borders in the shadows suggesting that the affected lung tissue was fibrotic. Similar findings have been reported previously (22, 23).

5.2. Computed Tomography Manifestations of Influenza Pneumonia

Some scholars are of the belief that the CT manifestations of influenza pneumonia are mainly diffuse or multiple small nodules, patchy, flaky GGO in unilateral or bilateral lung fields which may be accompanied by consolidation and mostly distributed around the bronchial vascular tree or under the pleura (24, 25). The CT manifestations in the lungs in this group of patients were basically consistent with the abovementioned suggestion since most lesions were multifocal (31 cases) and bilateral (25 cases). In this regard, the following manifestations were observed: lesion distribution along the bronchial blood vessels (n=15), lesion distribution under the pleura (n=12) , changes in shadows (n=14), simple changes (n=5), and an air bronchogram sign with changes in the shadows (n=16).

It is worth noting that five cases had mediastinal lymphadenopathy in this group which can be attributed to other pathogens (26). Some scholars believe that influenza pneumonia is rarely associated with pleural effusion, and the occurrence of pleural effusion might be related to underlying disease in these patients (27). Furthermore, three patients had pleural effusion in this group, including cardiac insufficiency (n=1), renal failure (n=1), and lung

cancer (n=1).

5.3. Identification of COVID-19 and Influenza Pneumonia

Both COVID-19 and influenza are acute respiratory infectious diseases caused by viruses. Concerning clinical symptoms, both diseases can cause fever, dry cough, and fatigue, and both show multiple lung lesions on CT. Nevertheless, COVID-19 is more common in the extrapulmonary zone under the pleura and can demonstrate the anti-butterfly wing sign. Influenza is distributed around the bronchial blood vessel tree or under the pleura. Both diseases can show different forms of simple GGO, mixed GGO, consolidation shadows, and thickened blood vessel shadows in the lesions. However, in the former, interlobular septal thickening are more common, and the air bronchogram sign appears earlier (28, 29). The latter shows a thicker lobular septum in the lesions, and the air bronchogram sign in the consolidation shadow appears later. When the lesions demonstrate mixed GGO, COVID-19 has fewer solid areas and slightly lower density in the lesions, while influenza has more solid areas and higher density as reported previously (30).

As a conclusion, chest HRCT demonstrated different characteristics of COVID-19 and influenza pneumonia and can be used as an important basis for the early detection and diagnosis of COVID-19 and influenza pneumonia. Therefore, it can be of paramount importance for the prevention and control of COVID-19.

6. Conclusion

The different chest HRCT features of COVID-19 and seasonal influenza pneumonia can provide considerable evidence for the early diagnosis of imported COVID-19 and seasonal influenza pneumonia and can be of great help for the prevention and control of COVID-19.

Acknowledgements

Our special appreciation goes to David Cushley (International Science Editing, Shannon, Ireland) for English language editing.

Footnotes

Authors' Contribution: Yuange Li and Yue Zhao performed the experiments and prepared the figures. Shiliang Long and Zhan Ge analyzed the results. Weiquan Wu and Jun Xia designed the research and wrote the paper. All authors read and approved the final manuscript.

Conflicts of interest: The authors declare that they have no conflict of interest regarding the publication of the current article.

Ethical Approval: Procedures were reviewed and approved by the Ethics Committee of Affiliated Hospital of Guangdong Medical University.

Funding/Support: The present study was supported by the Science and Technology Development Funds of Zhanjiang, Guangdong, China (2016C01016 and 2020B01009).

References

1. Wu F, Zhao S, Yu B, Chen YM, Wang W, Song ZG, et al. A new coronavirus associated with human respiratory disease in China. *Nature*. 2020;**579**(7798):265-9. doi: 10.1038/s41586-020-2008-3. [PubMed: 32015508].
2. Zhou F, Yu T, Du R, Fan G, Liu Y, Liu Z, et al. Clinical course and risk factors for mortality of adult inpatients with COVID-19 in Wuhan, China: a retrospective cohort study. *Lancet*. 2020; **395**(10229):1054-62. doi: 10.1016/S0140-6736(20)30566-3. [PubMed: 32171076].
3. Lu R, Zhao X, Li J, Niu P, Yang B, Wu H, et al. Genomic characterisation and epidemiology of 2019 novel coronavirus: implications for virus origins and receptor binding. *Lancet*. 2020;**395**(10224):565-74. doi: 10.1016/S0140-6736(20)30251-8. [PubMed: 32007145].
4. Lai CC, Shih TP, Ko WC, Tang HJ, Hsueh PR. Severe acute respiratory syndrome coronavirus 2 (SARS-CoV-2) and coronavirus disease-2019 (COVID-19): the epidemic and the challenges. *Int J Antimicrob Agents*. 2020;**55**(3):105924. doi: 10.1016/j.ijantimicag.2020.105924. [PubMed: 32081636].
5. Yuen KS, Ye ZW, Fung SY, Chan CP, Jin DY. SARS-CoV-2 and COVID-19: the most important research questions. *Cell Biosci*. 2020;**10**:40. doi: 10.1186/s13578-020-00404-4. [PubMed: 32190290].
6. Keilman LJ. Seasonal influenza (Flu). *Nurs Clin North Am*. 2019;**54**(2):227-43. doi: 10.1016/j.cnur.2019.02.009. [PubMed: 31027663].
7. Petrova VN, Russell CA. The evolution of seasonal influenza viruses. *Nat Rev Microbiol*. 2018;**16**(1):47-60. doi: 10.1038/nrmicro.2017.118. [PubMed: 29081496].
8. Webster RG, Govorkova EA. Continuing challenges in influenza. *Ann N Y Acad Sci*. 2014;**1323**(1):115-39. doi: 10.1111/nyas.12462. [PubMed: 24891213].
9. Henritzi D, Hoffmann B, Wacheck S, Pesch S, Herrler G, Beer M, et al. A newly developed tetraplex real-time RT-PCR for simultaneous screening of influenza virus types A, B, C and D. *Influenza Other Respir Viruses*. 2019;**13**(1):71-82. doi: 10.1111/irv.12613. [PubMed: 30264926].
10. To J, Torres J. Viroporins in the influenza virus. *Cells*. 2019; **8**(7):654. doi: 10.3390/cells8070654. [PubMed: 31261944].
11. Mahase E. Covid-19: WHO declares pandemic because of "alarming levels" of spread, severity, and inaction. *BMJ*. 2020;**368**:m1036. doi: 10.1136/bmj.m1036. [PubMed: 32165426].
12. Cucinotta D, Vanelli M. WHO declares COVID-19 a pandemic. *Acta Biomed*. 2020;**91**(1):157-60. doi: 10.23750/abm.v91i1.9397. [PubMed: 32191675].
13. Brody H. Influenza. *Nature*. 2019;**573**(7774):S49. doi: 10.1038/d41586-019-02750-x. [PubMed: 31534258].
14. Moriyama M, Hugentobler WJ, Iwasaki A. Seasonality of respiratory viral infections. *Annu Rev Virol*. 2020;In Press. doi: 10.1146/annurev-virology-012420-022445. [PubMed: 32196426].
15. Li Y, Yao L, Li J, Chen L, Song Y, Cai Z, et al. Stability issues of RT-PCR testing of SARS-CoV-2 for hospitalized patients clinically diagnosed with COVID-19. *J Med Virol*. 2020; **92**(7):903-7. doi: 10.1002/jmv.25786. [PubMed: 32219885].
16. Xie X, Zhong Z, Zhao W, Zheng C, Wang F, Liu J. Chest CT for typical 2019-nCoV pneumonia: relationship to negative RT-PCR testing. *Radiology*. 2020;**296**(2):E41-5. doi: 10.1148/radiol.2020200343. [PubMed: 32049601].
17. Ai T, Yang Z, Hou H, Zhan C, Chen C, Lv W, et al. Correlation of chest CT and RT-PCR testing in coronavirus disease 2019

(COVID-19) in China: a report of 1014 cases. *Radiology*. 2020;**296**(2):E32-40. doi: 10.1148/radiol.2020200642. [PubMed: 32101510].
18. Xiong Y, Sun D, Liu Y, Fan Y, Zhao L, Li X, et al. Clinical and high-resolution CT features of the COVID-19 infection: comparison of the initial and follow-up changes. *Invest Radiol*. 2020; **55**(6):332-9. doi: 10.1097/RLI.0000000000000674. [PubMed: 32134800].
19. Tanaka N, Emoto T, Suda H, Kunihiro Y, Matsunaga N, Hasegawa S, et al. High-resolution computed tomography findings of influenza virus pneumonia: a comparative study between seasonal and novel (H1N1) influenza virus pneumonia. *Jpn J Radiol*. 2012;**30**(2):154-61. doi: 10.1007/s11604-011-0027-6. [PubMed: 22180185].
20. Chung M, Bernheim A, Mei X, Zhang N, Huang M, Zeng X, et al. CT imaging features of 2019 novel coronavirus (2019-nCoV). *Radiology*. 2020;**295**(1):202-7. doi: 10.1148/radiol.2020200230. [PubMed: 32017661].
21. Amorim VB, Rodrigues RS, Barreto MM, Zanetti G, Hochhegger B, Marchiori E. Influenza A (H1N1) pneumonia: HRCT findings. *J Bras Pneumol*. 2013;**39**(3):323-9. doi: 10.1590/S1806-37132013000300009. [PubMed: 23857688].
22. Pan Y, Guan H, Zhou S, Wang Y, Li Q, Zhu T, et al. Initial CT findings and temporal changes in patients with the novel coronavirus pneumonia (2019-nCoV): a study of 63 patients in Wuhan, China. *Eur Radiol*. 2020;**30**(6):3306-9. doi: 10.1007/s00330-020-06731-x. [PubMed: 32055945].
23. Duan YN, Qin J. Pre- and posttreatment chest CT findings: 2019 novel coronavirus (2019-nCoV) Pneumonia. *Radiology*. 2020;**295**(1):21. doi: 10.1148/radiol.2020200323. [PubMed: 32049602].
24. Kim MC, Kim MY, Lee HJ, Lee SO, Choi SH, Kim YS, et al. CT findings in viral lower respiratory tract infections caused by parainfluenza virus, influenza virus and respiratory syncytial virus. *Medicine (Baltimore)*. 2016;**95**(26):e4003. doi: 10.1097/MD.0000000000004003. [PubMed: 27368011].
25. Ishiguro T, Takayanagi N, Kanauchi T, Uozumi R, Kawate E, Takaku Y, et al. Clinical and radiographic comparison of influenza virus-associated pneumonia among three viral subtypes. *Intern Med*. 2016;**55**(7):731-7. doi: 10.2169/internalmedicine.55.5227. [PubMed: 27041156].
26. El-Badrawy A, Zeidan A, Ebrahim MA. 64 multidetector CT findings of influenza A (H1N1) virus in patients with hematologic malignancies. *Acta Radiol*. 2012;**53**(6):662-7. doi: 10.1258/ar.2012.120038. [PubMed: 22734081].
27. Asai N, Suematsu H, Sakanashi D, Kato H, Hagihara M, Watanabe H, et al. A severe case of Streptococcal pyogenes empyema following influenza A infection. *BMC Pulm Med*. 2019;**19**(1):25. doi: 10.1186/s12890-019-0787-9. [PubMed: 30691434].
28. Zhou Z, Guo D, Li C, Fang Z, Chen L, Yang R, et al. Coronavirus disease 2019: initial chest CT findings. *Eur Radiol*. 2020; **30**(8):4398-406. doi: 10.1007/s00330-020-06816-7. [PubMed: 32211963].
29. Zhou S, Wang Y, Zhu T, Xia L. CT features of coronavirus disease 2019 (COVID-19) pneumonia in 62 patients in Wuhan, China. *AJR Am J Roentgenol*. 2020;**214**(6):1287-94. doi: 10.2214/AJR.20.22975. [PubMed: 32134681].
30. Kloth C, Forler S, Gatidis S, Beck R, Spira D, Nikolaou K, et al. Comparison of chest-CT findings of Influenza virus-associated pneumonia in immunocompetent vs. immunocompromised patients. *Eur J Radiol*. 2015;**84**(6):1177-83. doi: 10.1016/j.ejrad.2015.02.014. [PubMed: 25796425].